Quantitative reconstruction of summer precipitation using a Mid Holocene δ^{13}C common millet record from Guanzhong Basin, northern China

Qing Yang[1,2], Xiaoqiang Li[2]*, Xinying Zhou[2], Keliang Zhao[2] & Nan Sun[3]

1. School of Geography Science, Nanjing Normal University, Nanjing, 210023, China
2. Key Laboratory of Vertebrate Evolution and Human Origin of Chinese Academy of Sciences, Institute of Vertebrate Paleontology and Paleoanthropology, Chinese Academy of Sciences, Beijing, 100044, China
3. The School of Earth Science and Resources, Chang'an University, Xi'an, Sha'anxi, 710054, China

*Correspondence and requests for materials should be addressed to X.L. (lixiaoqiang@ivpp.ac.cn)

Abstract

To quantitatively reconstruct Holocene precipitation for particular geographical areas, suitable proxies and faithful dating controls are required. The fossilized seeds of common millet (*Panicum miliaceum*) are found throughout the sedimentary strata of northern China, and are suited to the production of quantitative Holocene precipitation reconstructions: their isotopic carbon composition (δ^{13}C) gives a measure of the precipitation required during the growing season of summer (here the interval from mid-June to September), and allows these seeds to be dated. We therefore used a regression function, as part of a systematic study of the δ^{13}C of common millet, to produce a quantitative reconstruction of Mid Holocene summer precipitation in the Guanzhong Basin (107°40′～107°49′N, 33°39′～34°45′N). Our results showed that mean summer precipitation at 7.7-3.4 ka BP was 353 mm, ～50 mm or 17% higher than present levels and the variability becomes increasing, especially after 5.2 ka BP. Maximum mean summer precipitation peaked at 414 mm during the period 6.1-5.5 ka BP, ~109 mm (or 36%) higher than today, indicating that the EASM peaked at this time. This work can provide a new proxy for further research into continuous paleoprecipitation sequences and the variability of summer precipitation, which will promote the further research into the relation between early human activity and environmental change.

Keywords: summer precipitation; quantitative reconstruction; Holocene; Chinese Loess Plateau; common millet; stable carbon isotope

Sect.

1 Introduction

The reconstruction of global climate changes through history is an important part of the Past Global Changes (PAGES) project. The Holocene, as the most recent geological period, has the closest relation to human survival and development. Quantitatively reconstructing climatic factors such as temperature and precipitation provides an understanding of agricultural development and the human impact upon

the landscape and environment. However, instrumental records are insufficient for the documenting of the drivers of climate change, since they cover only the past century or so (DeMenocal, 2001). The quantitative reconstruction of temperature and precipitation using climatic proxy records has therefore become the principal thrust of PAGES research. To date, most continental paleoclimate studies have focused on temperature (Porter and An, 1995; Guo *et al.*, 1996; Genty *et al.*, 2003; Wang *et al.*, 2008; Sun *et al.*, 2012). However, the increase in global surface temperatures has tended to cause changes in precipitation and atmospheric moisture through changes in atmospheric circulation, a more active hydrological cycle and an increasing water holding capacity throughout the atmosphere (Dore, 2005). The availability of water, one of the major challenges for the future, cannot be ignored, due to its significant role in the hydrological cycle (Hatté and Guiot, 2005). To this end, we chose an area key to the warm period of the Holocene to produce a quantitative precipitation reconstruction for that geological time.

The Chinese Loess Plateau (CLP), located in a transition zone between a semi-arid and semi-humid climate, is highly sensitive to changes in precipitation and has thus long been a key area for precipitation reconstruction research. The precipitation of the CLP, is, and has been, deeply impacted by the EASM. The EASM, an important component of the Asian Summer Monsoon (ASM), plays an indispensable role in the hydrological cycle over southern China. Various proxies have been adopted in studies of the EASM during the Holocene. Due to their reliable chronology and relatively easy dating, oxygen isotopes (δ^{18}O) in speleothems from Chinese caves have been taken as a robust measure of summer monsoon precipitation values (Wang *et al.*, 2005a; Cheng *et al.*, 2009). However, the interpretation of these changes in the δ^{18}O values of precipitation remains highly controversial; some scientists have contended that the stalagmite δ^{18}O record from the EASM region may not record EASM variability (Le Grande and Schmidt, 2009; Maher and Thompson, 2012; Tan, 2012; Caley *et al.*, 2014; Liu *et al.*, 2015). Fortunately, the precipitation in the CLP can effectively reflect the intensity of the EASM variability due to its special location (Liu et al., 2015).

The quantitative precipitation reconstruction results obtained have been based exclusively on climatic proxies derived from geological and biological records in the CLP. In the western CLP, fossil charcoal records in the Tianshui Basin have demonstrated that the mean annual precipitation (MAP) was 688-778 mm at 5.2-4.3 ka BP (Sun and Li, 2012). In the CLP's hinterland, magnetic susceptibility records from the Luochuan profile have provided estimates of Holocene MAP varying between 600 and 750 mm, with a mean value of 701±74 mm (Lu *et al.*, 1994). In the southern CLP, Guanzhong Basin MAP, as revealed by plant phytolith assemblies, was 700–800 mm during the Holocene, indicating a much more humid climate than today's (Lu *et al.*, 1996). Further evidence from the transfer functions of geological records and the intensity of pedogenesis has shown that Guanzhong Basin MAP was >700 mm during the Holocene Optimum (Sun *et al.*, 1999; Zhao, 2003), supporting the aforementioned results. However, due to their intrinsic limitations, such as discontinuity or an indefinite response mechanism between the proxies and

climate change, these tentative proxies have not been extensively applied. Selecting an effective proxy which evinces a reliable dating and a clear implication is crucial for the quantitative reconstruction of paleoprecipitation. High-resolution pollen-based quantitative precipitation results indicating EASM evolution have recently been obtained from an alpine lake in northern China (Chen *et al.*, 2015). However, because these are attributable solely to this unique environment, a regional quantitative precipitation reconstruction, and therefore a new proxy, is still required.

Common millet (*Panicum miliaceum*), as the most representative agricultural rain-fed crop of northern China, contains $\delta^{13}C$; this is sensitive to precipitation and can thus effectively record precipitation during the growing season (Yang and Li, 2015). Rain-fed agriculture originated in the CLP, giving rise to the first recognizably Chinese civilization. Many archeological relics from an unbroken historical continuum are therefore found throughout the region (An, 1988). Quantities of the fossilized seeds of common millet are well-preserved in the cultural layers of these archeological sites (Zhao and Xu, 2004; Liu *et al.*, 2008; Lu *et al.*, 2009). Their stable $\delta^{13}C$ compositions, which remain little change because of the low temperatures associated with carbonization, contain valuable information about paleoclimate change and early agricultural activities (Yang *et al.*, 2011a, 2011b). Common millet remains are therefore preferable for quantitatively reconstructing Holocene precipitation in the CLP.

The Guanzhong Basin (Figure 1), in the southern CLP, was the cradle of Neolithic culture and China's ancient civilization, and fostered the Laoguantai (~7.8-6.9 ka BP), Yangshao (~6.9-5.0 ka BP) and Longshan (~5.0-4.0 ka BP) cultures (Ren and Wu, 2010), the pre-Zhou culture (~3.5-3.0 ka BP) (Lei, 2010), and the Zhou dynasties. Due to the intensity of early agricultural activity, huge quantities of common millet remains have been preserved in numerous, continuously-occupied cultural sites. Charred common millet seeds are the most abundant resource found in the samples collected in this study from these cultural layers.

In this study, common millet remains, from five sections characterized by continuous and well-developed sedimentation at typical archeological sites, including the Baijia, Huiduipo, Manan, Beiniu and Nansha sites (Figure 1), were sampled as part of a systematic study of $\delta^{13}C$ records; quantitative precipitation reconstructions for the Holocene were then based upon a transfer function between the $\delta^{13}C$ of modern common millet and precipitation, providing a scientific basis for predicting future climate change and its possible impact.

2 The rationale behind using common millet $\delta^{13}C$ for precipitation reconstruction

The $\delta^{13}C$ values of common millet seeds reflect the ^{13}C of photosynthetic materials during not only their formative and mature stages, but also their vegetative stage. The growing season of modern common millet in the Guanzhong Basin lasts from June to September. The seed kernel's formative and mature stages occur soon after pollination of the blossom. With an increase in kernel size, photosynthetic material as well as pre-accumulated organic material is transferred to kernels from

stems, leaves and spikes (Chai, 1999). Therefore, millet $\delta^{13}C$ reflects the environmental conditions extant during the growing season from mid-June to the end of September, or 110 days in total.

Carbon isotope composition of fossilized plant remains is a useful proxy for the reconstruction of local paleoclimatic changes, especially when using $\delta^{13}C$ values from plants which experience a single mode of photosynthesis. Common millet grains have been widely and continuously preserved throughout the Holocene in northern China. Fossilized millet seeds were generally formed by baking at low temperatures (~250℃) (Yang *et al*., 2011a), and deposited in strata over long time periods with limited interaction with the buried environment. The observed $\delta^{13}C$ values of charred common millet formed at ~250℃ were 0.2‰ lower than those of the source samples, and much less than the natural variation typically found in wood (Yang *et al*., 2011b). The $\delta^{13}C$ signatures conserved in charred common millet are thus reflective of the true environment.

The carbon isotope composition of plants ($\delta^{13}C_p$) is affected by both physiological characteristics and environmental factors. The $\delta^{13}C$ of C_3 plants responds to environmental factors, such as atmospheric CO_2 pressure, O_2 partial pressure, temperature, light and precipitation, by dominating the ratio of the intercellular and ambient partial pressure of CO_2 (c_i/c_a) with the opening and closing of leaf stomata (Körner and Diemer, 1987; Körner and Larcher, 1988; Körner *et al*., 1989; Farquhar *et al*., 1989; Dawson *et al*., 2002). However, the $\delta^{13}C$ of C_4 plants depends not only on c_i/c_a but also on how much CO_2 and HCO_3^- in bundle sheath cells leaks into the mesophyll cells (called leakiness φ), which is determined by its physiological characteristics (Hubick *et al*., 1990). When φ is larger/smaller than 0.37, there is a positive/negative correlation between $\delta^{13}C_p$ and c_i/c_a (Ubierna *et al*., 2011). Under water stress, the φ of the common millet, belonging to the NADP-ME subgroup of C_4 plants, is likely larger than 0.37 (Schulze *et al*., 1996; Yang and Li, 2015). This may account for the significantly positive relation between the $\delta^{13}C$ of common millet and precipitation (Yang and Li, 2015).

Limited precipitation and soil humidity are the most important environmental factors affecting the growth of plants in arid and semi-arid areas (Hadley and Szarek, 1981; Ehleringer and Mooney, 1983; Murphy and Bowman, 2009). For C_4 species in the arid regions of northwestern China, $\delta^{13}C_p$ tends to decrease with decreasing soil water availability (Wang *et al*., 2005b). For common millet, although altitude, precipitation and water availability have a significant correlation with $\delta^{13}C$ according to correlation analysis, precipitation was the critical control of $\delta^{13}C$, based on functional mechanism analysis (Yang and Li, 2015). The plants' physiological characteristics and morphological adaptability showed that the stomatal, and some non-stomatal, factors of common millet are sensitive to water status, causing the $\delta^{13}C$ of the organic material to change with precipitation. This rationale establishes an important theoretical foundation whereby the $\delta^{13}C$ of common millet can serve as an effective indicator of paleoprecipitation.

3 Methods

Sampling. All the ancient common millet remains used in this study were found at five archeological sites in the Guanzhong Basin, *i.e.* the Baijia, Huiduipo, Manan Beiniu and Nansha sites (State Cultural Relics Bureau, 1998).

The Guanzhong Basin is located southern of the CLP and is bordered on the south by the Qinling Mountains and the north by the Beishan Mountain and spanned 30-80 km; from Baoji Valley at the west end to Tongguan at the east end, spanning 360 km. The topography is flat and the landscape consists mostly of river terraces and loess table land at an altitude of 326-600 m. The present-day Guanzhong Basin is characterized by semi-humid and semi-arid climatic conditions strongly influenced by the monsoon. Summer monsoon rainfall accounts for most of the annual precipitation and falls primarily in June-August; the climate is therefore characterized by cold, dry winters and moist, warm summers. Mean annual temperature (MAT) in the Guanzhong area is ca. 13℃, MAP is ~575 mm and mean annual relative humidity (MARH) is 70%. Precipitation data from the Guanzhong Basin for the period 1951-2011 were analyzed (Figure 2). The results showed that the precipitation for mid-June to September was between 110-526 mm, with a mean of 305 mm. The 95% confidence interval for this mean is between 279-332 mm, ruling out the extreme values of abnormal years.

The Baijia site, located on the secondary river terrace of the northern bank of River Wei, contains early Laoguantai cultural remains. The area is ca. 120,000 m^2 and the thickness of the cultural layer is between 0.4 m and 1.2 m. The Huiduipo site includes Banpo-type remains from the Yangshao culture. The area is ca. 60,000 m^2, the thickness of the cultural layer is ca. 2 m, and there is partial exposure of ash pits, residential areas and graves. The Manan site, located on tableland at the intersection of the Jinghe and Weihe rivers, exhibits Yangshao cultural remains. MN is ca. 16,000 m^2 in area, and the thickness of the cultural layer is between 2 m and 5 m, with a dense distribution of ash pits. The Beiniu site partly contains Longshan cultural remains. Its area is 200,000 m^2, and the thickness of its cultural layer is ca. 1m. The Nansha site is mainly characterized by Shang Dynasty remains. It is ca. 300,000 m^2 in area and the thickness of its cultural layer is between 1.9 m and 2.7 m (State Cultural Relics Bureau, 1998). All sampling sections are described in Figure 1.

Five sections characterized by continuous and well-developed sedimentation were selected for sampling at the Baijia, Beiniu, Huiduipo, Manan and Nansha sites. The slice sampling were applied to continuously sampling and the interval was 10 cm for the Baijia and Nansha sections, and 20 cm for the Beiniu, Huiduipo and Manan sections (Figure 1). Forty litre sample bags were filled with sufficient quantities of sedimentary material to screen through a 50-mesh sieve to obtain samples using flotation (Tsuyuzaki, 1994). Different archeological remains were separated in the laboratory after air-drying. Agricultural seeds were identified and picked out under the stereomicroscope, then marked in order according to sampling depth. The number of remnant common millet samples derived from all five sections are listed in Table 1.

Stable $\delta^{13}C$ analysis. Stable $\delta^{13}C$ composition analyses were carried out on all 67 serial and bulk common millet samples from the five sections, each composed of three to five grains, without lemma. Each sample portion was placed in a beaker and covered with a 1% hydrochloric acid solution to remove any carbonates. The samples were then washed with deionized water to pH >5 and oven dried at 40°C for 24 h. The dried samples were ground in an agate mortar and homogenized, then vacuum-sealed in a quartz tube with copper oxide and silver foil and combusted for at least 4 h at 850°C. The CO_2 gas from the combustion tube was extracted and cryogenically purified. The isotopic ratio of the extracted CO_2 gas was determined using a MAT-253 gas source mass spectrometer with a dual inlet system at the Institute of Earth Environment, Chinese Academy of Sciences.

All isotope ratios were expressed using the following δ notation:

$$\delta^{13}C(‰) = [(R_{sample} - R_{std})/R_{std}] \times 1000 \qquad \text{Eq. (1)}$$

The isotopic standard used was Vienna Pee Dee Belemnite (VPDB); analytical precision at the 1σ level was reported as 0.2‰.

Radiocarbon dating. AMS ^{14}C dating was conducted on one charcoal fragment and one charred seed of common millet from the Baijia section, five charred seeds each from the Huiduipo and Beiniu sections, one charred seed from the Manan section, and three charred seeds from the Nansha section.

The charcoal and seed samples were pretreated by washing in 10% NaOH and 10% HCl and reduced to neutral pH. They were then converted to graphite and radiocarbon ages were calculated after measurement in the STAR Accelerator at the Australian Nuclear Science and Technology Organisation (ANSTO). AMS ^{14}C dates were calibrated using Calib Rev 7.0.4 software and the INTCAL13 dataset (Reimer *et al.*, 2013).

Processing data of age model. On the basis that the depth-based linear interpolation method was not fit for the dating of cultural layers because of potential disturbance, all common millet remnant samples were divided into several groups to guarantee at least one dating dataset for each group (Figure 3a), as follows: samples from adjacent depths with close $\delta^{13}C$ values were placed in the same group, allowing a greater difference between each group (One-factor Analysis of Variance (one-way ANOVA), P<0.05).

Quantitative modeling method and data analysis. The results for $\delta^{13}C$ values in the seeds of modern millet grown on the CLP (Yang and Li, 2015) demonstrated that the $\delta^{13}C$ of common millet has a significant positive correlation with precipitation. In this study, standard major axis regression analysis (SMA) was applied to establish a regression model between the $\delta^{13}C$ of modern common millet and precipitation during growing seasons. Statistical analyses were conducted using SMATR software (Version 2.0) (Falster *et al.*, 2006). Other statistical analyses used SPSS 15.0 for Windows and OriginPro 8.0 software. Unless otherwise stated, differences were considered statistically significant when P<0.05.

4 Results

The radiocarbon results (Table 2) show that the ages of the sampled cultural

layers were usually correspondent with archeological periodization. Common millet remains sampled from cultural layers of Guanzhong Basin in our study have $\delta^{13}C$ values ranging from -11.1‰ to -9.3‰ (Figure 3a), with a mean of -10.2±0.4‰ (n＝66, SD=±1 σ), without considering the anomaly value of -8.8‰ analyzed by Boxplot using SPSS statistical software (Figure 3b), which may be affected by the local environment. The $\delta^{13}C$ composition of modern common millet from the central and western CLP measured in 2008 ranged from -13.9‰ to -12.5‰, with a mean of -13.2±0.5‰ (n＝15, SD=±1σ) (Yang and Li, 2015). It can thus be seen that the $\delta^{13}C$ values of common millet remains are more positive than those of modern millet by ～2.9‰.

The ^{13}C composition of plants results from a combination of carbon isotope fractionation and source carbon isotope composition. Therefore, $\delta^{13}C$ changes in the atmosphere, as a part of total CO_2, are an important factor impacting upon the $\delta^{13}C$ values in plants (O'Leary, 1988; Farquhar, 1989; Araus and Buxo, 1993). Considering our atmosphere is a perfect blender, we adopted the global mean $\delta^{13}C$ value of atmospheric CO_2, -8.2%, in 2011 (Cuntz, 2011), which was three years after sampling. The $\delta^{13}C$ values of atmospheric CO_2 in the Holocene, from 11 ka BP to the pre-industrial age, show only a slight change, usually ranging between -6.1‰ and -6.6‰, with a mean value of -6.4± 0.15‰ (Marino *et al*., 1992; Leuenberger *et al*., 1992). ～1.8‰ higher than present-day atmospheric CO_2 $\delta^{13}C$ values of -8.2‰ (Farquhar *et al*., 1989; Keeling and Whorf, 1992). After correcting for the change in atmospheric CO_2 $\delta^{13}C$ (1.8‰), the millet $\delta^{13}C$ values for Holocene millet from the Guanzhong Basin are equivalent to modern caryopsis values of -12.0±0.4‰, and are therefore ～1.2‰ less depleted in $\delta^{13}C$ than modern caryopsis (for the t test, t=21.39).

The regression function between $\delta^{13}C$ and precipitation for the common millet growing season was established using SMA as follows (Figure 4):

$$\delta^{13}C(‰)= 0.0077P_{gs}-14.76,r^2 = 0.56,P＜0.001 \qquad Eq.(2)$$

Where P_{gs} denotes the precipitation of millet growth seasons. The function's gradient indicated that the precipitation coefficient was 0.77‰/100 mm, implying that, within physiological adaptation parameters, there would be a ~0.77‰ increase in $\delta^{13}C$ with a 100 mm increase in precipitation. The $\delta^{13}C$ values yielded by ancient common millets are higher than those of modern common millet seeds, suggesting that these ancient plants grew in a more humid environment than today's.

Common millet remains from archeological sites were divided into a total of 11 groups (Table 3). Mean $\delta^{13}C$ values for common millet remains were calculated for each group. Results showed that the minimum value was -10.6±0.2‰, and the maximum value -9.6±0.1‰, for common millet growing between 7.7 ka BP and 3.4 ka BP. After correcting for the change in the atmospheric CO_2 $\delta^{13}C$ (1.8‰), the range of mean $\delta^{13}C$ values for ancient millet *vis-à-vis* modern plants was between -12.4±0.2‰ and -11.4±0.1‰. By applying the regression model based on the $\delta^{13}C$ and precipitation values for modern common millet during its growing season, we were able to extract paleoprecipitation values for the growing seasons of ancient crops for certain time periods.

These paleoprecipitation values were reconstructed by applying the corrected

δ^{13}C values for the ancient millet to the regression equation (Eq. 2) which expresses the relation between the δ^{13}C of common millet and precipitation. The results showed that the precipitation for the growing seasons of ancient millet during the period 7.7-3.4 ka BP varied from 240 mm to 477 mm, with a mean of 354 mm (Table 3).

5 Discussion

Ancient equivalent-seed δ^{13}C values, ranging from -12.4±0.2‰ to -11.4±0.1‰, are ～1–2‰ higher than those for modern millet in the area. Paleoprecipitation reconstructed from the regression function shows that precipitation of millet growth seasons at 7.7-3.4 ka BP was between 242 and 475 mm, with a mean of 353 mm. Summer paleoprecipitation values show that the climate was much more humid than it is today, which was 305 mm on average during 1951-2011, with mean precipitation ~50 mm, or 17%, higher. A peak mean summer precipitation of 442 mm was reached at ~5.7 ka BP; even the lowest value of 311 mm ~6.5 ka BP was higher than today's mean value. Summer precipitation during the Mid Holocene (7.7-3.4 ka BP) in the Guanzhong Basin exhibited a systemic increase.

The reconstructed summer precipitation also fluctuates significantly and becomes more and more variable, especially after 5.2 ka BP. However, there were three markedly humid periods, i.e. 6.1-5.5 ka BP, ~4.2 ka BP, and ~3.6 ka BP (Figure 5). The period 6.1-5.5 ka BP had the most abundant summer precipitation, which was 414 mm, i.e. 109 mm, or 36%, higher than today. At ~4.1 ka BP, the precipitation was 397±11 mm, 92 mm or 30% higher than at present; at ~3.6 ka BP, the precipitation was 414±45 mm, 36% higher than at present.

The period 6.1-5.5 ka BP, being the most markedly humid period, probably marks the Holocene Climate Optimum in the Guanzhong Basin; this was also when the Yangshao Culture flourished, with archeological finds indicating that there were as many villages in the area as there are today. It is worth noting that the anomalous high value at ~4.1 ka BP and ~3.6 ka BP, may indicate rapidly-developing climatic events, correspondent with other global records (Cullen and DeMenocal, 2000; Mayewski et al., 2004; Wu and Liu, 2004).

The instrumental data for the last 61 years (1951-2011) indicate that precipitation in the Guanzhong Basin occurs mainly in the summer (Figure 2). The current inland flow of warm/humid air dominated by the EASM during the summer (June through September) delivers ~58% of the total annual precipitation. The area is a typical monsoon precipitation area, and summer precipitation here is therefore sensitive to variations in the EASM.

Previous studies of various climatic proxies including stalagmite δ^{18}O, lacustrine sediments and loess-paleosols all indicate that the CLP had plenty of rain in the Holocene and was much more humid during the Mid Holocene (Shen *et al*., 2005; Wang *et al*., 2005a; Wang *et al*., 2008; Wang *et al*., 2014; Chen *et al*., 2015). The frequency of paleosol development increased during ~8.6-3.2 ka in the CLP (Wang *et al*., 2014). The eolian-sand activities in the sandlands located to the north of the CLP decreased from ~8.6-3.2 ka BP (Wang *et al*., 2014; Yang *et al*., 2012), whilst the vegetation coverage of the desert/loess transitional zone increased in this interval

(Yang *et al*., 2015). These various proxy records infer that the EASM was stronger during the Mid Holocene, but the amplitude of any variations in the EASM remains difficult to assess.

Our quantitative reconstructions of summer precipitation based on millet $\delta^{13}C$ indicate that EASM intensity peaked during 6.1-5.5 ka BP. The strongest summer monsoon brought the wettest millet growth seasons, with 36% higher precipitation than today's. More evidence supporting our contention comes from the tree pollen records from lake sediments around the CLP, which respond more directly to changes in the EASM than the other records because trees on the margins of monsoonal regions are sensitive to variations in monsoonal precipitation. Pollen records from Qinghai Lake, located to the west of the Guanzhong Basin and on the modern monsoon margins, indicate a wet interval during 7.4-4.5 ka BP, culminating in a peak at 6.5 ka BP (Figure 6a) (Shen *et al*., 2005). Although the increase in precipitation cannot be assessed, the general trend is comparable with our $\delta^{13}C$-based precipitation reconstruction results. The percentage of broadleaf trees from pollen record in the Gonghai Lake (on the northeastern margins of the CLP; Figure 6b), indicate that the peak monsoonal period occurred during ~7.8-5.3 ka BP, with an average annual precipitation of 574 mm (Figure 6c), ~30% higher than the modern value (Chen *et al*., 2015). The increase in precipitation is highly consistent with our reconstruction results. More evidence from PMIP2 (the second phase of the Paleoclimate Modeling Intercomparison Project) coupled with Mid Holocene simulations showed that the summer precipitation associated with the EASM increased throughout most of China ~6 ka BP and the greatest increases in precipitation seen in the region, *i.e.* the southern margins of the Tibetan Plateau, and southeastern coastal area of China, which experienced precipitation increases of >1.5 mm/day and 0.7 mm/day (or 547.5 mm/yr and 255.5 mm/yr), respectively (Zhang and Liu, 2009). According to the result, it can be inferred the increase in precipitation in the Guanzhong Basin was lower than 255.5 mm/yr at that time. These multiple lines of evidence corroborate our reconstructions, not only *vis-à-vis* changes in precipitation during the Holocene, but also their quantitative accuracy.

5 Conclusions

$\delta^{13}C$ of common millet from archaeological layer can effectively record precipitation during millet growing season. Summer precipitation at 7.7-3.4 ka BP reconstructed using the $\delta^{13}C$ values of common millet was 353 mm, ～50 mm, or 17%, higher than at present. Maximum mean summer precipitation peaked at 414 mm during the period 6.1-5.5 ka BP, ~109 mm (or 36%) higher than today, indicating that the EASM peaked at this time. Furthermore, the increasing variability of summer precipitation was visible, especially after 5.2 ka BP. The work provides a new proxy for establishing the paleoprecipitation record.

Charred common millet remains continuously exist in the archaeological layers since around 10 ka in northern China. Not only the common millet can provide a reliable dating framework, but also the continuous $\delta^{13}C$-based paleoprecipitation sequences could be quantitatively reconstructed. This, in turn, can allow regional

comparisons, providing a scientific foundation for promoting further research and helping to understand the processes and mechanisms of the EASM, as well as the relation between early human activity and environmental change.

Authorial contributions

X. Q. L.: overall coordination of writing, sampling, ^{14}C dating and paleoprecipitation reconstruction; Q. Y.: writing, sampling, data processing and paleoprecipitation reconstruction; X. Y. Z. and K. L. Z.: sampling and data processing; N. S.: sampling and ^{14}C dating. All authors reviewed the manuscript.

Acknowledgements

This study was supported by the National Basic Research Program of China (Grant No. 2015CB953804, 2015CB953803), the National Natural Science Foundation of China (Grant Nos. 41301042, 41372175) and the National Science Fund for Talent Training in Basic Science (Grant No. J1210008). We thank Prof. John Dodson for AMS[14]C dating support, and Dr. Ying Xi for assistance with collecting the original meteorological data.

References

An, Z. M.: Prehistoric agriculture in China, Acta. Archaeol. Sin., 4, 369–381, in Chinese, 1988.

Araus, J. L., and Buxo, R. Changes in carbon isotope discrimination in grain cereals from the north-western Mediterranean Basin during the past seven millennia, Aust. J. Plant. Physiol., 20, 117-128, 1993.

Caley, T., Roche, D. M. and Renssen, H.: Orbital Asian summer monsoon dynamics revealed using an isotope-enabled global climate model, Nat. Commun., 5, 5371, 2014.

Chai, Y.: Broomcorn millet, Chinese Agriculture Press, Beijing, China, 47-70, 1999.

Chen, F. H., Xu, Q. H., Chen, J.H., Birks, H. J. B., Liu, J. B., Zhang, S. R., Jin, L., An, C. B., Telford, R. J., Cao, X. Y., Wang Z. L., Zhang, X. J., Selvaraj, K., Lu, H. Y., Li, Y.C., Zheng, Z., Wang, H. P, Zhou, A.F., Dong, G.H., Zhang, J. W., Huang, X. Z., Bloemendal, J., and Rao, Z.G.: East Asian summer monsoon precipitation variability since the last deglaciation, Sci. Rep., 5, 11186, 2015.

Cheng, H., Edwards, R.L., Broecker, W. S., Denton, G.H., Kong, X., Wang. Y., Zhang, R., Wang, X.: Ice Age Terminations, Science, 326, 248-252, 2009.

Cullen, H. M, deMenocal, P. B.: North Atlantic influence on Tigris-Euphrates stream flow, International Journal of Climatology, 20, 853-863, 2000.

Cuntz, M.: Carbon cycle: A dent in carbon's gold standard, Nature, 477, 547–548, 2011.

Dawson, T.E., Mambelli, S., Plamboeck, A. H., Templer, P. H., and Tu, K. P.: Stable Isotopes in Plant Ecology, Annu. Rev. Ecol. Syst., 33, 507–559, 2002.

DeMenocal, P. B.: Cultural responses to climate change during the late Holocene, Science, 292, 667-673, 2001.

Dore, M. H. I.: Climate change and changes in global precipitation patterns: What do we know?, Environ. Int., 31, 1167-1181, 2005.

Ehleringer, J. R., and Mooney, H. A.: Photosynthesis and productivity of desert and Mediterranean climate plants, Encyclopedia Plant Physiol (NS), Springer-Verlag, New York, 205-231, 1983.

434   Falster, D. S., Warton, D. I., and Wright, I. J.: User's guide to SMATR: Standardised Major Axis
435   Tests & Routines Version 2.0, Copyright 2006, 2006,
436   http://www.bio.mq.edu.au/ecology/SMATR/

437   Farquhar, G. D., Ehleringer, J. R., and Hubick, K. T.: Carbon isotope discrimination and
438   photosynthesis, Annu. Rev. Plant Physiol. Mol. Biol., 40, 503-537, 1989.

439   Genty, D., Blamart, D., Ouahdi, R., Gilmour, M., Baker, A., Jouzel, J., Van-Exter, S.: Precise
440   dating of Dansgaard–Oeschger climate oscillations in western Europe from stalagmite data,
441   Nature, 421, 833-837, 2003.

442   Guo, Z. T., Liu, T., Guiot, J., Wu, N., L, H., Han, J., Liu, J., Gu, Z.: High frequency pulses of East
443   Asian monsoon climate in the last two glaciations: link with the North Atlantic, Clim. Dynam,
444   12, 701-709, 1996.

445   Hadley, N.F., and Szarek, S.R.: Productivity of desert ecosystems, BioScience, 31, 747-753, 1981.

446   Hatté, C., and Guiot, J.: Palaeoprecipitation reconstruction by inverse modelling using the isotopic
447   signal of loess organic matter: application to the Nußloch loess sequence (Rhine Valley,
448   Germany), Clim Dynam, 25, 315-327, 2005.

449   Hubick, K.T., Hammer, G. L., Farquhar, G. D., Wade, L. J., von Caemmerer, S., and Henderson, S.
450   A.: Carbon isotope discrimination varies genetically in C4 species, Plant. Physiol., 92, 534–537,
451   1990.

452   IPCC: Climate Change 2007: The Physical Science Basis, Solomon, S. et al. Cambridge, 2007

453   Keeling, C. D., and Whorf, T. P. in: Atmospheric CO_2 – modern record, Mauna Loa, edited by:
454   Boden, T A, Sepanski, R. J. and Stoss, F. W.: Trends 91: A Compendium of Data on Global
455   Change, ORNL/CDIAC-46, Carbon Dioxide Information Analysis Center, Oak Ridge National
456   Laboratory, Oak Ridge, Tennessee, USA, 12-15, 1992.

457   Körner, C. H., and Diemer, M.: *In situ* photosynthetic responses to light, temperature and carbon
458   dioxide in herbaceous plants from low and high altitude, Funct. Ecol., 1(3), 179-194, 1987.

459   Körner, C. H., and Larcher, W. Plant life in cold climates, Symp Soc Exper Biol., 42, 25–57,
460   1988.

461   Körner, C. H., Newmayer, M., Palaez Menendez-Reidl, S., and Smeets-Scheel, A.: Functional
462   morphology of mountain plants, Flora, 182, 353-383, 1989.

463   LeGrande, A., and Schmidt, G.: Sources of Holocene variability of oxygen isotopes in
464   paleoclimate archives, Clim. Past, 5, 441-455, 2009.

465   Lei, X. S.: Pre-Zhou culture exploration, Science Press, Beijing, China, in Chinese, 2010.

466   Leuenberger, M., Siegenthaler, U., and Langway, C. C.: Carbon isotope composition of
467   atmospheric CO_2 during the last ice age from an Antarctic ice core, Nature, 357, 488-490, 1992.

468   Liu, C. J., Jin, G. Y., and Kong, Z. C.: Archaeobotany — Research on Seeds and Fruits, Science
469   Press, Beijing, China, pp. 160-171, 2008.

470   Liu, J.B., Chen, J.H., Zhang, X. J., Li, Y., Rao, Z. G., and Chen, F. H.: Holocene East Asian
471   summer monsoon records in northern China and their inconsistency with Chinese stalagmite
472      $\delta^{18}O$ records, Earth-Sci. Rev., 148, 194-208, 2015.

473   Lu, H. Y., Han, J. M., Wu, N. Q., and Guo Z. T.: The analysis of modern soil magnetic
474   susceptibility and its paleoclimate significance, Sci. China, Ser. B, 24(12), 1290-1297, in
475   Chinese, 1994.

476   Lu, H. Y., Wu, N. Q., Liu, T. S., Han, J. M., and Qin X. G.: Seasonal climatic variation recorded
477   by phytolith assemblages from the Baoji loess sequence in central China over the last 150 000,

478   Sci. China, Ser. D, 39(6), 629-639, 1996.

479   Lu, H. Y., Zhang, J. P., Liu, K.-B., Wu, N. Q., Li, Y. M., Zhou, K. S., Ye, M. L., Zhang, T. Y.,

480   Zhang, H. J., Yang, X. Y., Shen, L. C., Xu, D. K., Li, Q., and Piperno, D. R.: Earliest

481   domestication of common millet (*Panicum miliaceum*) in East Asia extended to 10,000 years

482   ago, P. Natl. Acad. Sci. U.S.A., 18, 7367-7372, 2009.

483   Maher, B. A., and Thompson, R.: Oxyen isotopes from Chinese caves: records not of monsoon

484   rainfall but of circulation regime, J. Quat. Sci., 27, 615-624, 2012.

485   Marino, B. D., McElroy, M. B., Salawitch, R. J., and Spaulding, W. G.: Glacial-to-interglacial

486   variations in the carbon isotopic composition of atmospheric CO_2, Nature, 357, 461-466, 1992.

487   Mayewski, P. A., Rohling, E. E., Stager, J. C., Karlén, W., Maasch, K. A., Meeker, L. D.,

488   Meyerson, E. A., Gasse, F., van Kreveld, S., Holmgren, K, Lee-Thorp, J., Rosqvist, G., Rack,

489   F., Staubwasser, M., Schneider, R. R., and Steig, E. J.: Holocene climate variability, Quatern.

490   Res., 504 62(3), 243-255, 2004.

491   Murphy, B. P., and Bowman, D. M. J. S.: The carbon and nitrogen isotope composition of

492   Australian grasses in relation to climate, Funct Ecol, 23, 1040–1049, 2009.

493   O'Leary, M. H.: Carbon isotopes in photosynthesis, BioScience, 38, 323-336, 1988.

494   Porter, S. C., and An, Z. S.: Correlation between climate events in the North Atlantic and China

495   during the last glaciation, Nature, 375, 305-308, 1995.

496   Reimer, P. J., Bard, E., Bayliss, A., Beck, J. W., Blackwell, P. G., Ramsey, C. B., Buck, C. E., Hai

497   C., Edwards, R. L., Friedrich, M., Grootes, P. M., Guilderson, T. P., Haflidason, H., Hajdas, I.,

498   Hatté, C., Heaton, T. J., Hoffmann, D. L., Hogg, A. G., Hughen, K. A., and Kaiser, K. F.:

499   IntCal13 and Marine13 radiocarbon age calibration curves 0-50,000 years cal BP, Radiocarbon

500   55(4), 1869-1887, 2013.

501   Ren, S. N., and Wu, Y. L.: The Neolithic Volume of Chinese Archaeology, Chinese Social Science

502   Press, Beijing, China, in Chinese, 2010.

503   Schulze, E.-D., Ellis, R., Schulze, W., Trimborn, P., and Ziegler, H.: Diversity, metabolic types

504   and $\delta^{13}C$ carbon isotope ratios in the grass flora of Namibia in relation to growth form,

505   precipitation and habitat conditions, Oecologia, 106, 352-369, 1996.

506   Shen, J., Liu, X. Q., Wang, S. M., and Ryo, M.: Palaeoclimatic changes in the Qinghai Lake area

507   during the last 18,000 years, Quat. Int., 136, 131-140, 2005.

508   State Cultural Relics Bureau (ed): Atlas of Chinese Cultural Relics: Shannxi Municipality, Xi'an

509   Map Press, Xi'an, China, in Chinese, 1998.

510   Sun, J. M., Diao, G. Y., Wen, Q. Z., and Zhou, H. Y.: A preliminary study on quantitative

511   estimate of Palaeoclimate by using geochemical transfer function in the Loess Plateau,

512   Geochim, 28(3), 265-272, in Chinese, 1999.

513   Sun, N., Li, X. Q., Dodson, J., Zhou, X. Y., Zhao, K. L., Yang, Q.: Plant diversity of the Tianshui

514   Basin in the western Loess Plateau during the mid-Holocene – charcoal records from

515   archaeological sites, Quatern. Int, 308-309, 27-35, 2012.

516   Sun, N., and Li, X. Q.: The quantitative reconstruction of the palaeoclimate between 5200 and

517   4300 cal yr BP in the Tianshui Basin, NW China, Clim. Past, 8, 625-636, 2012.

518   Tan, M.: Circulation effect: response of precipitation $\delta^{18}O$ to the ENSO cycle in monsoon

519   regions of China, Clim. Dyn., 42, 1067-1077, 2012.

520   Tsuyuzaki, S.: Rapid seed extraction from soils by a flotation method, Weed Res., 34, 433-436,

521   1994.

Ubierna, N., Sun, W., and Cousins, A. B.: The efficiency of C_4 photosynthesis under low light conditions: assumptions and calculations with CO_2 isotope discrimination, J. Exp. Bot., 1–16, 2011.

Wang, H., Chen, J., Zhang, X., and Chen, F.: Palaeosol development in the Chinese Loess Plateau as an indicator of the strength of the East Asian summer monsoon: Evidence for a mid-Holocene maximum, Quaternary International, 334, 155-164, 2014.

Wang, Y. J., Cheng H., Edwards, R. L., He Y. Q., Kong, X. G., An, Z. S., Wu, J. Y., Kelly, M. J., Dykoski, C. A., and Li, X. D.: The Holocene Asian monsoon: links to solar changes and North Atlantic climate, Science, 308, 854-857, 2005a.

Wang, G.A., Han, J. M., Zhou, L. P., Xiong, X. G, and Wu, Z. H.: Carbon isotope ratios of plants and occurrences of C_4 species under different soil moisture regimes in arid region of Northwest China, Physiol.Plant., 125, 74–81, 2005b.

Wang, Y. J., Cheng, H., Edwards, R. L., Kong, X. G., Shao, X. H., Chen, S. T., Wu, J. Y., Jiang, X. Y., Wang, X. F., and An, Z. S.: Millennial- and orbital-scale changes in the East Asian monsoon over the past 224,000 years, Nature, 451, 1090-1093, 2008.

Warton, D. I., Wright I. J., Falster, D. S., and Westoby, M.: Bivariate Line-fitting methods for allometry, Biol. Rev., 81, 259-291, 2006.

Wu, W. X., Liu, T. S.: Possible role of the "Holocene Event 3" on the collapse of Neolithic Cultures around the Central Plain of China, Quaternary International, 117, 153-166, 2004.

Yang, Q., Li, X. Q., Zhou, X.Y., Zhao, K. L., Ji, M., and Sun, N.: Investigation of the ultrastructural characteristics of foxtail and broomcorn millet during carbonization and its application in archaeobotany, Chinese. Sci. Bull, 56(14), 1495-1502, 2011a.

Yang, Q., Li, X. Q., Liu, W. G., Zhou, X.Y., Zhao, K. L., and Sun, N.: Carbon isotope fractionation during low temperature carbonization of foxtail and common millets, Org. Geochem., 42, 713-719, 2011b.

Yang, L. H., Wang, T., Zhou, J., Lai, Z. P., and Long, H.: OSL chronology and possible forcing mechanisms of dune evolution in the Horqin dunefield in northern China since the Last Glacial Maximum, Quatern. Res., 78, 185-196, 2012.

Yang, Q., and Li, X. Q.: Investigation of the controlled factors influencing carbon isotope composition of foxtail and common millet on the Chinese Loess Plateau, Sci. China Ser D, 58(12), 2296-2308, 2015.

Yang, Q., Li, X.Q., and Zhou, X.Y.: Vegetation Succession Responding to Climate Changes since LGM in Desert-Loess Transition Zone, North China, Acta. Antherop. Sin., DOI: 10.16359/j.cnki.cn11-1963/q.2015.0000, in Chinese with English abstract , 2015.

Zhang, R and Liu, X. D.: An analogy analysis of summer precipitation change patterns between mid-Holocene and future climatic warming scenarios over East Asia, Sci. Geogr. Sin., 29(5), 679-683, in Chinese with English abstract, 2009.

Zhao, J. B.: Soil developed in the Holocene Megathermal and climatic migration in the Guanzhong area, Sci. Geogr. Sinia, 23(5), 554-559, 2003. (in Chinese with English abstract).

Zhao, Z. J., and Xu L. G.: The tentative flotation result and preliminary analysis in Zhouyuan ruins (Wangjiazui site), Cult. Rel., (10), in Chinese, 89-96, 2004.

Tables

Table 1 Sampling sites and the number of common millet samples

Sites	Location	Cultural types	Sample source	n
Baijia	34°33′7.53″N 109°24′38.6″E	Early Laoguantai Culture	Cultural layer	12
Huiduipo	34°34′4.1″N 109°01′41.8″E	Banpo type, Yangshao Culture	Cultural layer	9
Manan	34°28′23.7″N 109°05′17.5″E	Miaodigou type, Yangshao Culture	Cultural layer	11
Beiniu	109°19′2.6″E	Longshan Culture	Cultural layer	15
Nansha	34°29′30.1″N 109°42′47.9″E	Erlitou Culture, Shang Dynasty	Cultural layer	20

n means the number of remnant common millet samples derived from the section.

Table 2 Accelerator mass spectrometry (AMS) dates from Baijia (BJ), Huiduipo (HDP), Manan (MN), Beiniu (BN), and Nansha (NS)

Sample code	Depth (cm)	Sample type	Radiocarbon age (^{14}C yr BP)	Calibrated age range (cal yr BP, 2σ)	Lab code
BJ-15	180-190	Common millet	6,705± 40	7,504-7,657	OZM447
BJ-2	50-60	Charcoal	6,675±40	7,476-7,612	OZM446
HDP-13	235-250	Common millet	5,720±50	6,408-6,639	OZM473
HDP-9	160-180	Rice seed	5,015±45	5,655-5,896	OZM472
HDP-5	80-100	Rice seed	5,120±35	5,750-5,831	OZM471
HDP-3	40-60	Foxtail millet	5,185±40	5,891-6,009	OZM470
MN-8	140-160	Foxtail millet	4,550±35	5,053-5,191	OZM452
BN-13	280-300	Foxtail millet	5,450±70	6,172-6,400	OZM481
BN-10	220-240	Foxtail millet	3,820±45	4,138-4,360	OZM480
BN-8	180-200	Rice seed	3,770±35	4,073-4,244	OZM479
BN-5	120-140	Foxtail millet	4,540±50	5,040-5,323	OZM478
BN-1	40-60	Common millet	4,110±40	4,521-4,730	OZM477
NS-15	230-240	Wheat seed	3,300±30	3,454-3,593	OZM460
NS-11	200-210	Wheat seed	3,280±35	3,445-3,587	OZM459
NS-5	140-150	Wheat seed	3,300±30	3,454-3,593	OZM458

All assays were run on the STAR Accelerator, ANSTO, Australia. Calibrations refer to the Radiocarbon Calibration Program (Reimer et al., 2013).

Table 3 Information for grouped common millet remains, by section

Section	Cultural age	Depth (cm)	n	Calibrated ages (cal yr BP)	Mean δ^{13}C(‰)	Corrected δ^{13}C (‰)	P$_{gs}$ (mm)
Baijia	Laoguantai Culture	50-190	12	7,476-7,657	-10.4±0.2	-12.2±0.2	336±30
Huiduipo	Banpo type, Yangshao Culture	200-250	3	6,408-6,639	-10.6±0.3	-12.4 ±0.3	311±37
	Banpo type, Yangshao Culture	120-200	2	5,655-5,896	-9.6±0.1	-11.4 ±0.1	442±9

Site	Culture	Depth	n	Age	$\delta^{13}C$	Corrected $\delta^{13}C$	P_{gs}
	Banpo type, Yangshao Culture	0-120	5	5,750-6,009	-9.9±0.1	-11.7±0.1	402±12
Manan	Miaodigou type, Yangshao Culture	0-260	11	5,053-5,191	-10.3±0.4	-12.1±0.4	346±47
Beiniu	Yangshao Culture	260-300	3	6,172-6400	-10.3±0.1	-12.1±0.1	349±8
	Longshan Culture	180-240	3	4,073-4,360	-9.9±0.1	-11.7±0.1	397±13
	Longshan Culture	80-180	4	5,040-5,323	-10.3±0.2	-12.1±0.2	352±27
	Longshan Culture	40-80	4	4,521-4,730	-10.6±0.2	-12.4±0.2	313±22
Nansha	Erlitou Culture, Shang Dynasty	50-300	20	3,445-3,593	-10.2±0.4	-12.0±0.4	346±47

575 *n* means the number of samples for $\delta^{13}C$ analysis. Corrected $\delta^{13}C$ means $\delta^{13}C$ value of millet being

576 corrected the $\delta^{13}C$ difference of atmospheric CO_2 between modern and Holocene for precipitation

577 reconstruction. P_{gs} means reconstructed precipitation of millet growth seasons.

578 **Figures**

580
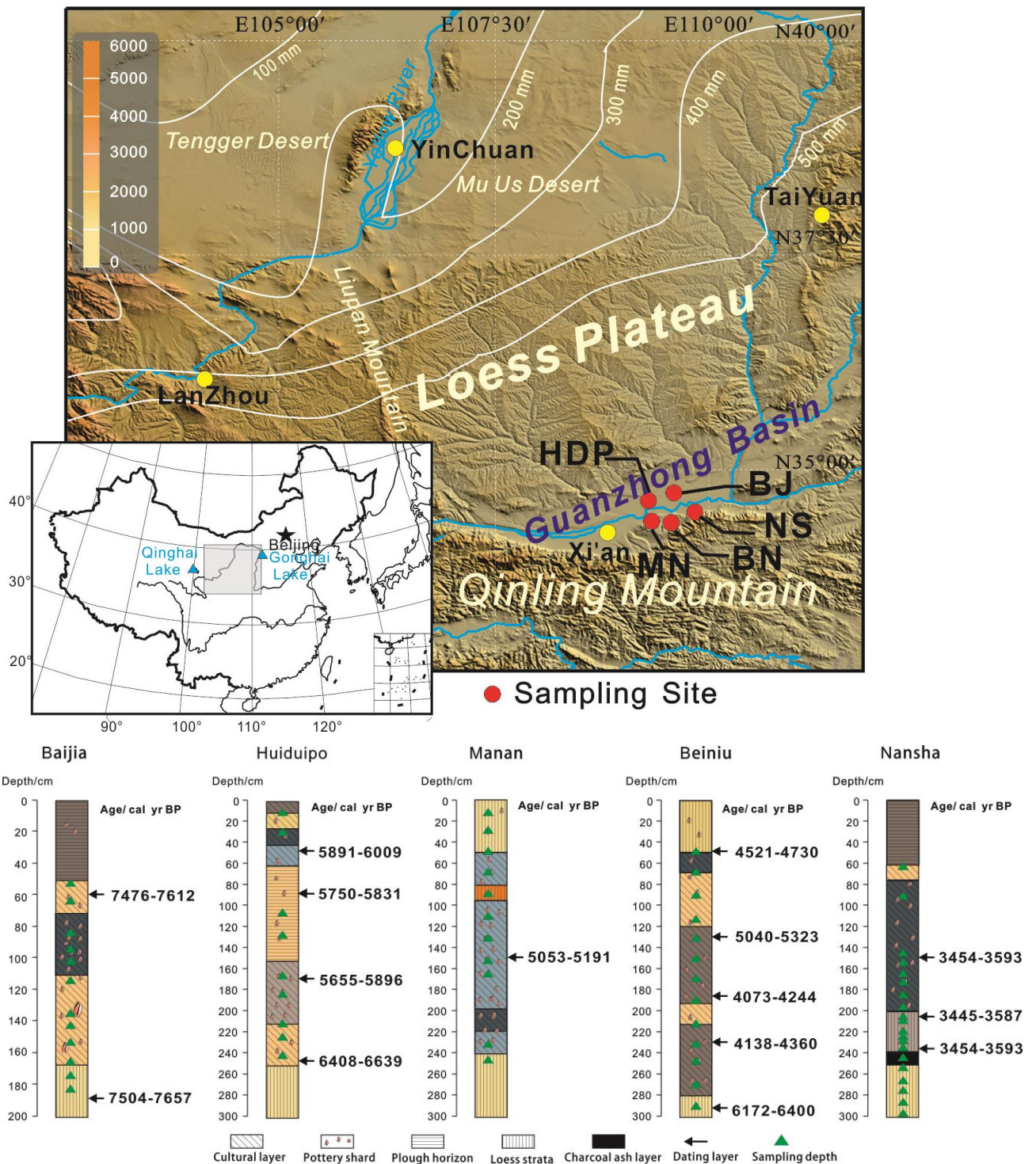
581 **Figure 1.** Location of sampling sites and description of all sampling sections. Red solid circles
582 indicate sampling sites: Baijia(BJ), Huiduipo (HDP), Manan (MN), Beiniu (BN), Nansha (NS).

583

584
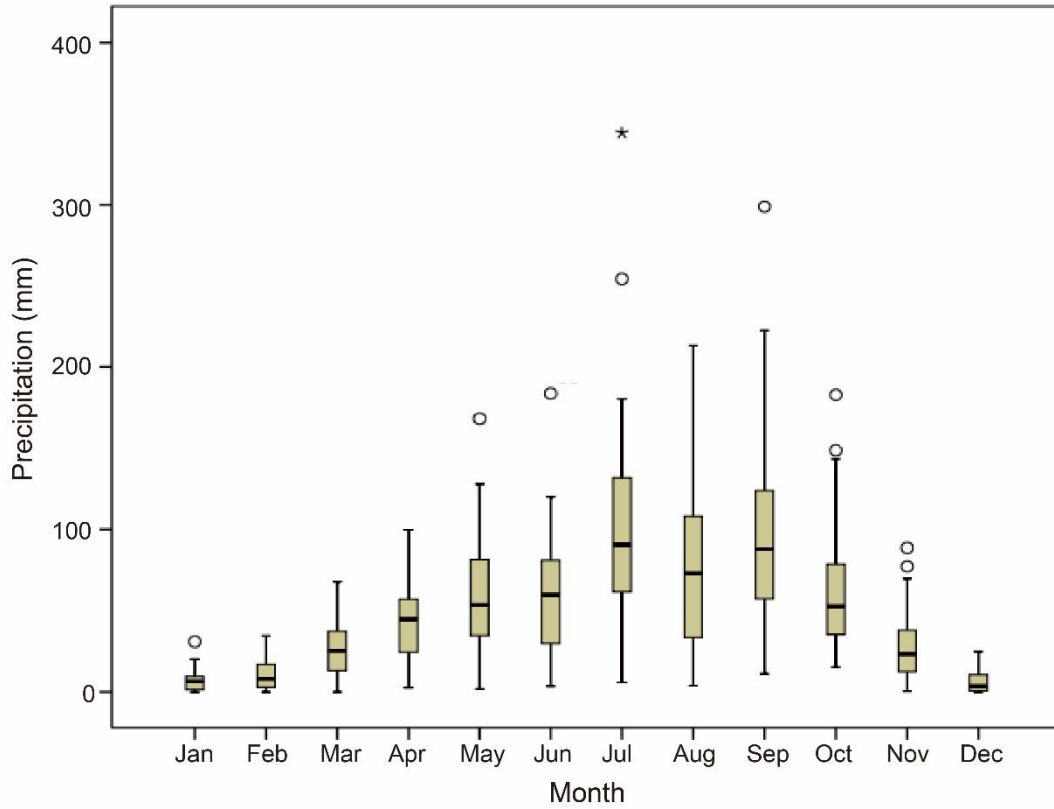
Figure 2. Instrumental precipitation data for 1951-2011 from Xi'an Station, Shaanxi, China
(original data, Data Sharing Platform, China Meteorological Administration). The empty circle (○)

indicates an abnormal value; the asterisk (*) indicates an extremely abnormal value.

588
589

590
591

592
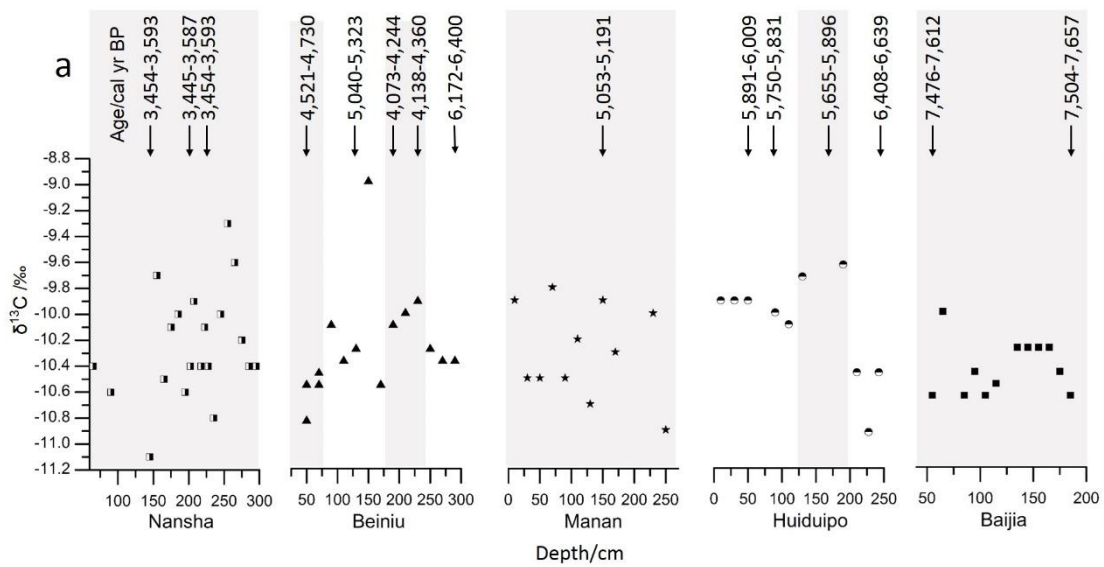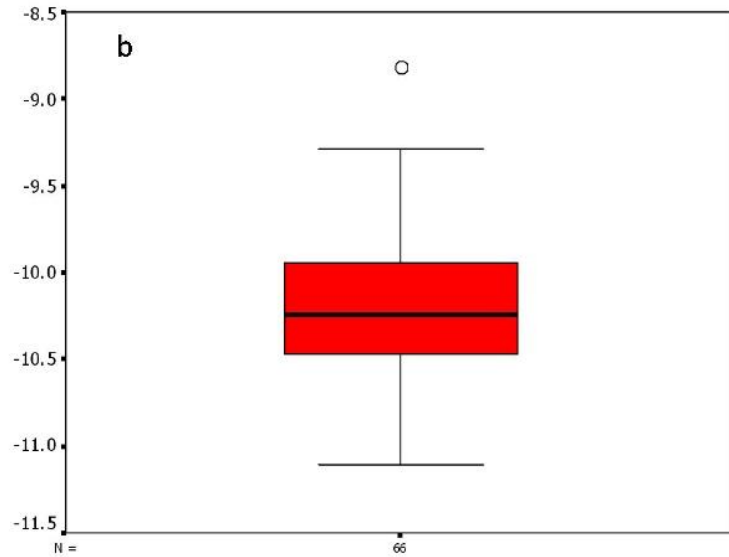
593 **Figure 3.** δ¹³C of common millet from archeological sites, Guanzhong Basin. Panel a shows raw

594 data points including all δ¹³C and calibrated age range versus depth. The group division were

595 expressed in gray or white color. Panel b shows Boxplot of all δ¹³C of common millet, with the

596 mean value 10.2±0.4‰ (n＝66, SD=±1 σ) and the anomaly value of -8.8‰ excluded.

597

598
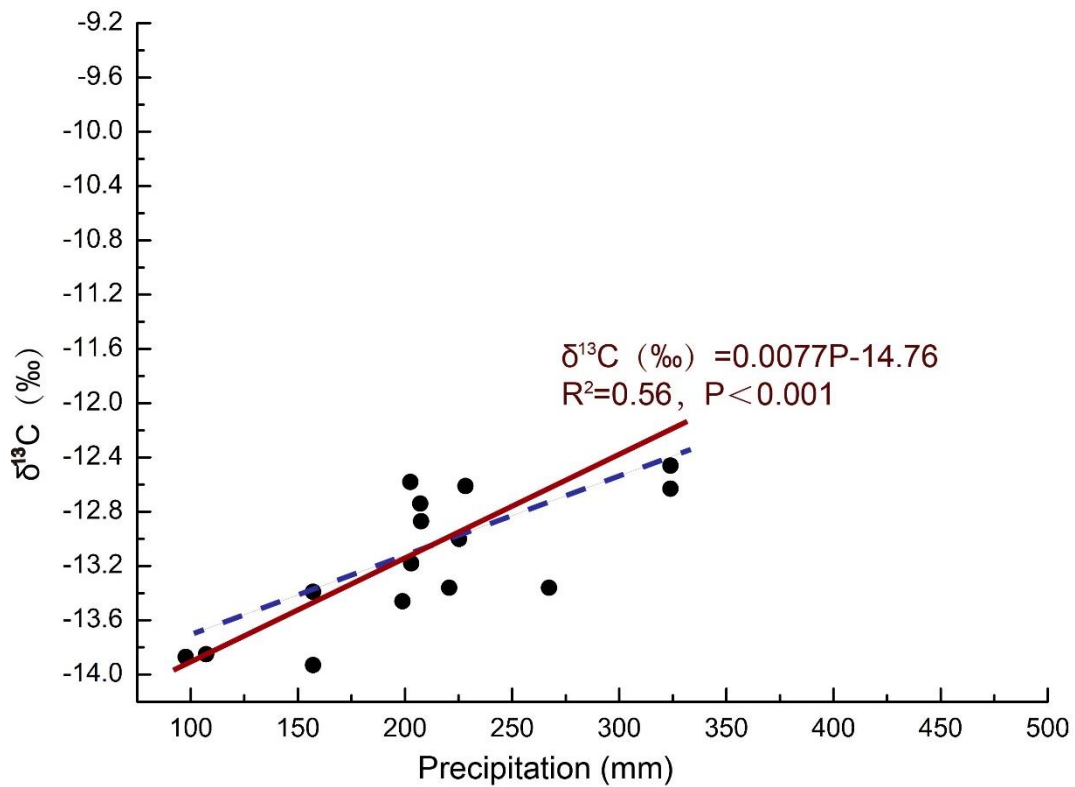
599 **Figure 4.** The regression model of the δ¹³C of modern common millet and summer precipitation,

600 which data from Yang and Li (2015). Dark red line denotes the line of best fit established using

601 SMA; the blue dotted line denotes the line of best fit established using OLS.

602

603

604

605
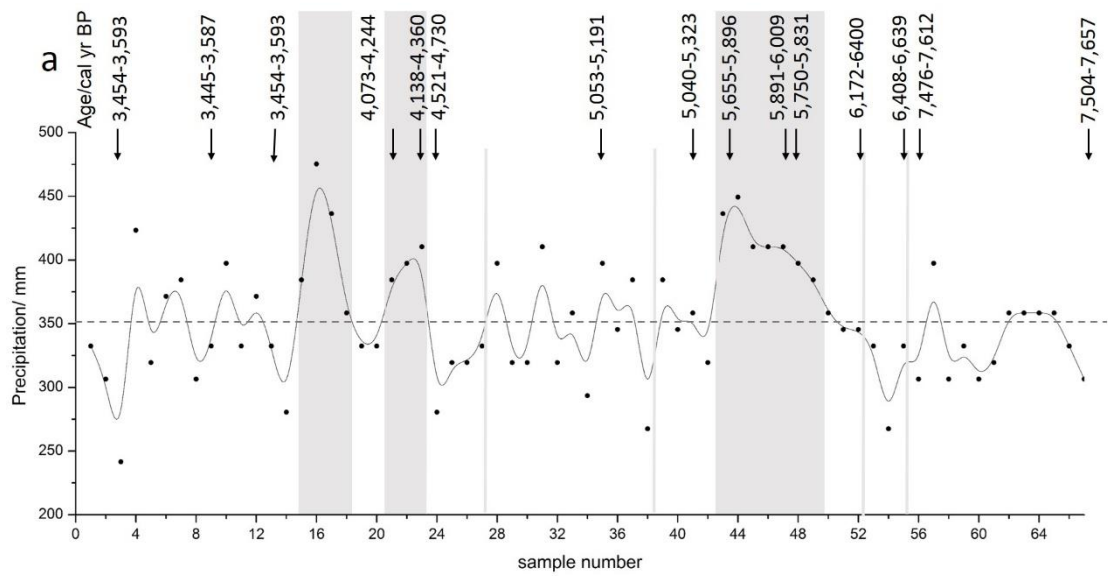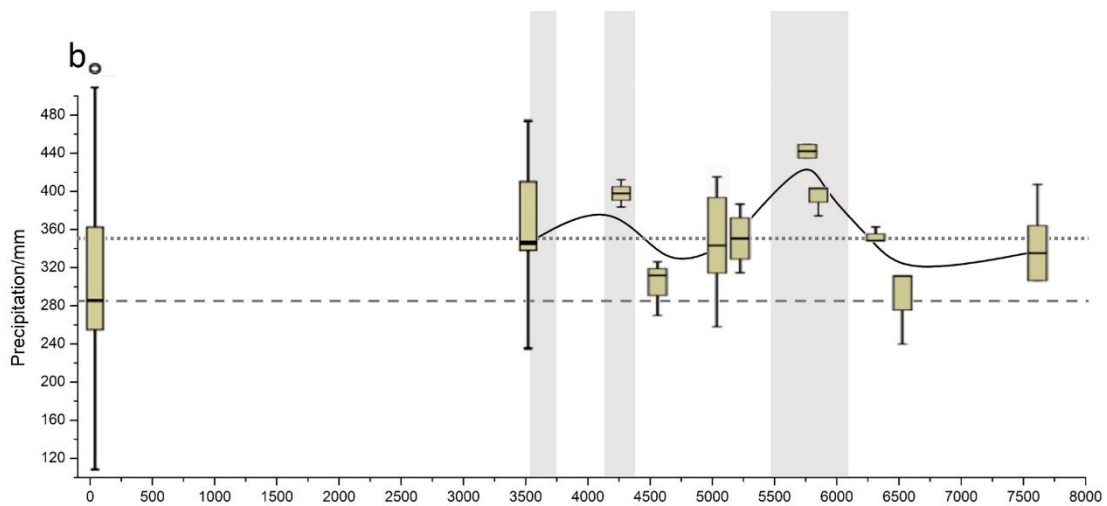
606 **Figure 5.** Reconstructed summer precipitation during 7.7-3.4 ka BP, Guanzhong Basin (Panel a)
607 and comparison the reconstructed precipitation during the Holocene to precipitation for mid-June
608 to September for a modern period in Xi'an city (original data for 1951–2011, from the China
609 Meteorological Administration). The gray color in both panel a and b indicates the markedly
610 humid periods during the Holocene. The gray line in panel a means the group division. The dot
611 line in panel b indicates the mean precipitation of millet growth season at 7.7-3.4 ka BP; the dash
612 line in panel b indicates the mean precipitation for mid-June to September during 1951-2011.

613

614

615
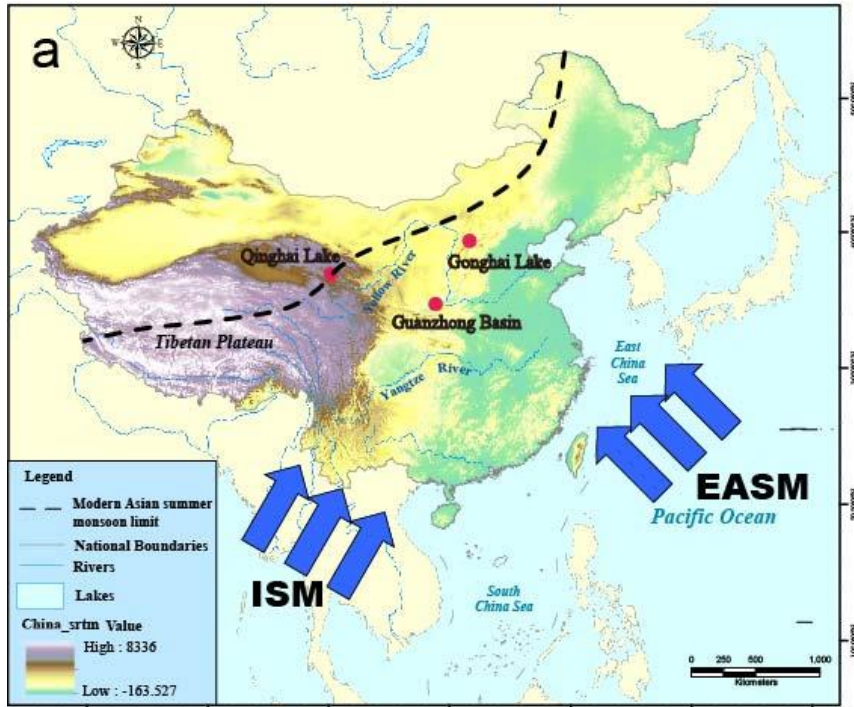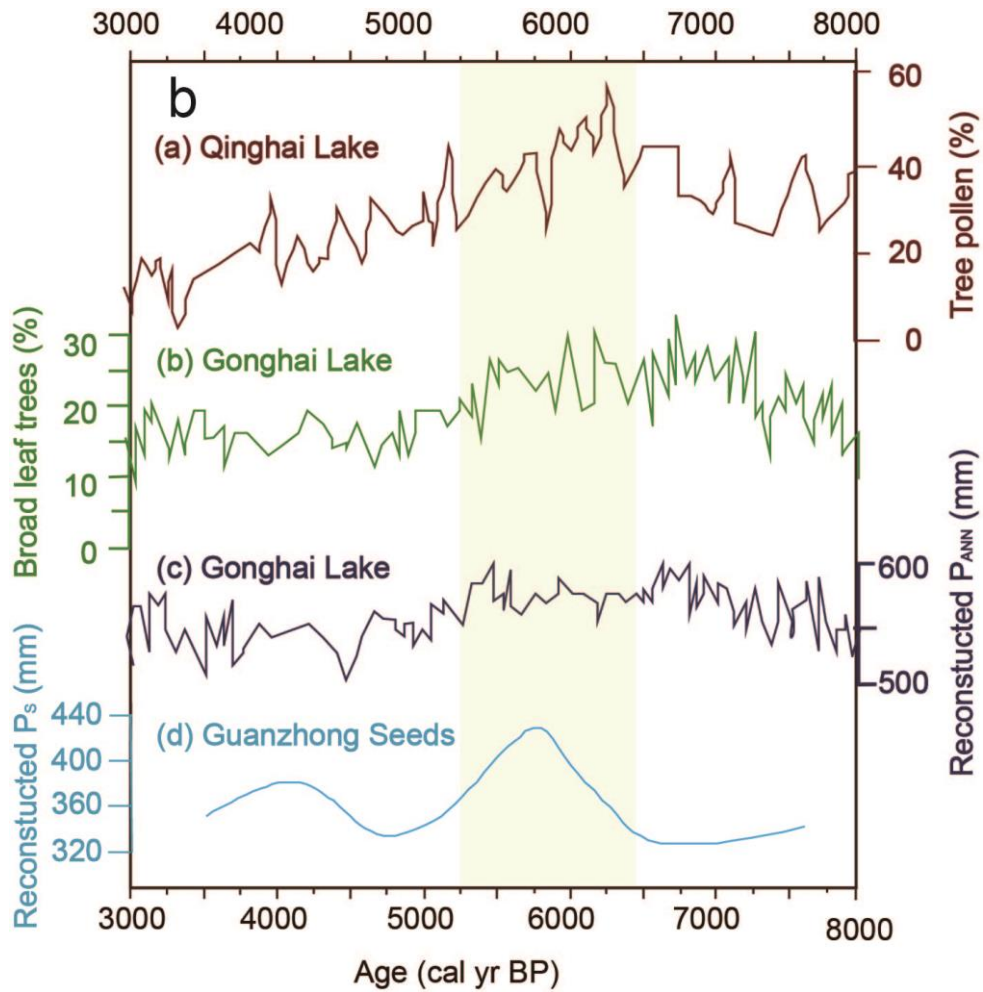
Figure 6. The modern Asian summer monsoon limit is shown by a dashed line in the map (panel

a). The red dots signed in the map are the locations of Qinghai Lake, Gonghai Lake and

618 Guanzhong Basin, whose precipitation were carried out comparison. Comparison of reconstructed

619 summer precipitation for 7.7-3.4 ka BP, Guanzhong Basin, with the pollen records of lakes

620 sediments from around the CLP. (**a**) Tree pollen percentages from Qinghai Lake (Shen *et al.*,

621 2005). (**b**) Broadleaf tree pollen percentages from Gonghai Lake (Chen *et al.*, 2015). (**c**)

622 Reconstructed annual precipitation from the pollen records of Gonghai Lake (Chen *et al.*, 2015).

623 (**d**) Reconstructed summer precipitation from the $\delta^{13}C$ values of common millet, Guanzhong

624 Basin.

625